Simulation of single-file ion transport with the lattice Fokker-Planck equation

Simone Melchionna
Department of Physics, INFM-SOFT, University of Rome, "La Sapienza," P.le A. Moro 2, 00185 Rome, Italy

Sauro Succi
Istituto per le Applicazioni del Calcolo "A. Picone," CNR, Viale del Policlinico 137, 00166 Rome, Italy

Jean-Pierre Hansen
Department of Chemistry, Lensfield Road, Cambridge CB2 1EW, United Kindgom
(Received 22 July 2005; revised manuscript received 21 October 2005; published 31 January 2006)

A lattice version of the Fokker-Planck equation, accounting for dissipative interactions, not resolved on the molecular scale, is applied to the study of electrorheological transport of a one-dimensional charged fluid, and is found to yield quantitative agreement with a recent analytical solution.

DOI: 10.1103/PhysRevE.73.017701 PACS number(s): 47.11.−j

Over the last decade discrete lattice versions of kinetic equations, most notably the Lattice-Boltzmann (LB) method, have undergone burgeoning progress for the simulation of large scale hydrodynamic flows [1–4] and of the dynamics of colloidal suspensions [5,6]. One of the major appeals of the LB method is its flexibility, which allows us to accommodate a host of complex physical effects, including boundary conditions at interfaces, intermolecular forces, and even chemical reactions, through efficient and elegant discretizations of the force term in the kinetic Vlasov-Boltzmann equation. One of the limitations of the LB method is that, since it generates the time evolution of the one-particle distribution function, fluctuations are not accounted for. "Brownian noise" becomes increasingly important as one explores flows on ever smaller scales, as in colloidal systems, or in narrow pores (microfluidics). Here we show that the LB methodology can be easily extended to deal with small scale processes involving a Brownian component, by introducing a lattice version of the Fokker-Planck (FP) collision operator [7,8]. In analogy with the LB equation, the present lattice Fokker-Planck equation builds upon an optimized form of importance sampling of velocity space which, at a variance with numerical grid methods [8–10], permits us to solve the Fokker-Planck equation near local equilibrium in single-particle phase space.

In this work an implicit solvent kinetic model is applied to the problem of single-file ion transport through a water-filled pore connecting two reservoirs, under the action of an applied electric field or ion-concentration gradient. The one-dimensional kinetic model provides a crude representation of ion permeation of ion channels through membranes separating intra- and extra-cellular compartments [11,12]. Ion permeation of such channels has been examined by numerous molecular dynamics or Brownian dynamics simulations of realistic or semirealistic quasicylindrical models (for a review, see [13]) or by numerical solutions of the Poisson-Nernst-Planck equations [14], but the present study is inspired by the recent kinetic modeling of Ref. [12]. The action of the confining, quasicylindrical pore is crudely represented by restricting ion motion to one dimension and by a contribution to the frictional force $-\gamma v$.

In one dimension, the time evolution of the distribution function $f=f(x,v;t)$ of a given particle is governed by the Fokker-Planck equation

$$(\partial_t + v\partial_x)f = C^{FP}[f] - a\partial_v f = \partial_v[\gamma(vf + v_T^2\partial_v f)] - a\partial_v f, \tag{1}$$

where $v_T=\sqrt{kT/m}$ is the thermal velocity and $a=qE/m$, E being the applied electric field and q the charge of the ions; in practice one is mostly interested in mono or divalent cations ($q=+e$ or $+2e$). The local equilibrium solution of the kinetic equation (1) is hence

$$f^{eq}(x,v;t) = [n(x;t)/(2\pi v_T^2)^{1/2}]e^{-[v-u(x;t)]^2/2v_T^2}. \tag{2}$$

The zeroth, first, and second moments of the distribution are the local density n, current J, and pressure (or momentum flux) P per unit mass and are given by

$$n(x;t) = \int_{-\infty}^{\infty} f(x,v;t)dv, \tag{3}$$

$$J(x;t) = \int_{-\infty}^{\infty} vf(x,v;t)dv \equiv n(x;t)u(x;t), \tag{4}$$

$$P(x;t) = \int_{-\infty}^{\infty} vvf(x,v;t)dv. \tag{5}$$

Note that in one dimension the momentum flux is proportional to the (kinetic) energy, but this is, of course, no longer true in higher dimensions.

By multiplying both sides of the kinetic equation (1) successively by 1, v, and v^2, and integrating over all v, one easily arrives at the following macroscopic moment equations:

$$\partial_t n(x;t) + \partial_x J(x;t) = 0, \tag{6}$$

$$\partial_t J(x;t) + \partial_x P(x;t) = -\gamma J(x;t) + n(x;t)a, \tag{7}$$

$$\partial_t P(x;t) + \partial_x Q(x;t) = -\gamma n(x;t)u^2(x;t) + 2aJ(x;t). \quad (8)$$

Equation (6) is the continuity equation expressing the conservation of mass; Eq. (7) expresses momentum balance with a proper account of friction and acceleration due to the electric field while (8) is the energy balance equation, taking into account the heat flux $Q(x;t)=\int_{-\infty}^{\infty} v^3 f(x,v;t)dv$ as well as frictional dissipation.

Many analytical and numerical procedures are available to solve the moment equations (6)–(8), [8]. In the following, however, we concentrate on a discrete kinetic representation of the distribution function $f(x,v,t)$ in which the space-time dependent fields $f_i(x,t)$, rather than being obtained through an integration over velocity degrees of freedom, retain instead a local meaning in velocity space. The space-time evolution of these discrete fields is governed by the following lattice-Fokker-Planck (LFP) equation [15]:

$$f_i(x + v_i\Delta t; t + \Delta t) - f_i(x;t) = \sum_j c_{ij}(x;t) f_j(x;t)\Delta t. \quad (9)$$

In the above $f_i(x;t)$ is the probability of finding a particle with discrete speed v_i at point x and time t, and

$$c_{ij}(x;t) = w_i \sum_k A_{ki} C_k(x;t) A_{kj} \quad (10)$$

is a collision matrix between discrete populations f_i and f_j. The quantities A_{ki} are orthonormal eigenvectors associated with the Hermite polynomials $h_k(v)$ (see Appendix) and C_k are the spectral coefficients of the FP operator, defined as

$$C_k(x,t) = \int C^{FP}[f(x,v;t)]h_k(v)dv. \quad (11)$$

Finally, Δt is the time step chosen for the numerical solution.

We consider a discretized model involving three discrete velocities $v_0, v_1, v_2 = 0, +1, -1$ and associated weights $w_0, w_1, w_2 = \frac{2}{3}, \frac{1}{6}, \frac{1}{6}$, with thermal speed $v_T^2 = \frac{1}{3}$. For this model, from (11), one readily computes $C_0 = 0$, $C_1 = -\gamma J + na$ and $C_2 = -2\gamma(P - nv_T^2) + 2aJ$.

Equation (9) corresponds to a first-order time integration of the corresponding time-continuous discrete Fokker-Planck equation, along the characteristics $\Delta x_i = v_i \Delta t$. The formulation of second-order time-marching schemes along the lines developed for the case of diagonal matrices, such as the lattice Bhatnagar-Gross-Krook equation, is left for future work [16,17]. A thorough Chapman-Enskog analysis of the macroscopic limit of Eq. (9) will be presented in a forthcoming detailed publication [18]. As an application of the LFP formalism, we consider the single-file transport of ions through a pore of length L connecting two reservoirs containing ions at given concentrations. As in Ref. [12] we assume that at both ends of the pore, the ion distribution function is a Maxwell-Boltzmann equilibrium distribution at temperature T which determines the thermal velocity v_T. The analytical solution for this case is given by

$$n_{exact}(x) = Ae^{a^* x/L} + B,$$

$$J_{exact} = aB/\gamma,$$

where

$$A = [1/2 \sinh(a^*/2)][n_r - n_l + (a^*/\gamma^*)\sqrt{2\pi}B],$$

$$B = n_l e^{a^*/2} - n_r e^{-a^*/2} / \left\{ 2\sinh(a^*/2) e^{-a^{*2}/2\gamma^{*2}} + \sqrt{\frac{\pi}{2}}\frac{a^*}{\gamma^*}\left[\cosh(a^*/2) + \sinh(a^*/2) \int_{-v_T a^*/\gamma^*}^{v_T a^*/\gamma^*} dv\, \Phi(v) \right] \right\},$$

and $\Phi = \sqrt{1/2\pi v_T} \exp(-v^2/2v_T^2)$. It should be appreciated that, even though the solution is a plain exponential, the competition between the effect of the boundary conditions and the driving electric field is reflected in a strongly nonlinear dependence of the current on the electric field (see the expression of B, which represents corrections to pure Ohmic behavior). This competition leads to a saturation, since the reservoirs cannot feed more than nv_T ions per unit area and time. As a result, the current cannot exceed its ballistic value $v_T n/\sqrt{2\pi}$ in the limit $E \to \infty$.

Numerical boundary conditions are imposed as follows:

$$f_1(x=0;t) = f_2(x=0;t) = [n_l - f_0(x=0;t)]/2,$$

$$f_0(x=0;t) = w_0 n_l, \quad (12)$$

where subscripts 1 and 2 stand for rightward and leftward propagation and n_l indicates the left reservoir density. At the right-end reservoir, open flow conditions are applied. The reservoirs are located at $x=0$ and $x=L+1$, respectively, while the physical channel runs from $1 \leqslant x \leqslant L$. Note that the expression (12) corresponds to fixing the incoming *flux* from the reservoir, hence it does not imply that n_l coincides with the fluid density at the inlet.

We define the dimensionless current $J^* = J\sqrt{2\pi/v_T^2}1/n$ the dimensionless acceleration, or electric field $a^* = maL/k_BT = qEL/k_BT = E/E_T$ and the dimensionless collision rate $\gamma^* = \gamma L/v_T = \gamma/\gamma_T = E_\gamma/E_T$ where n is the reservoir ion density, $E_T = k_BT/qL$ is a "thermal" electric field, such that the work it produces to move a charge q over the channel length L equals the thermal energy k_BT, while $E_\gamma = \gamma k_BT/(qv_T) = m\gamma v_T/q$ is the electric field producing on a charge q a force which balances the frictional force $-m\gamma v_T$. In other words, in a linear regime, the drift velocities associated with E_T and E_γ are $u_E = v_T/\gamma^*$ and $u_E = v_T$, respectively. Clearly, in infinitely long channels, or zero-temperature fluids, $u_T \to 0$, and the ionic current is controlled by pure dissipation, $u_E = qE/m\gamma$. In finite-size, finite-temperature situations, and constant-flux boundary conditions, however, deviations from this simple Ohmic regime must be expected, as we shall show below.

We have solved the LFP equation numerically to determine the stationary distribution function $f(x,v)$ and derive the corresponding macroscopic moments, primarily the current $J(x)$. In Fig. 1 the steady-state currents vs the field strength are shown for three values of the friction $\gamma^* = 20, 50, 100$, over a wide range of field amplitudes a^*, and compared with the analytical solution. The simulation is performed with $n_l = n_r = 1$ and $N = 10\,000$ grid points. From this

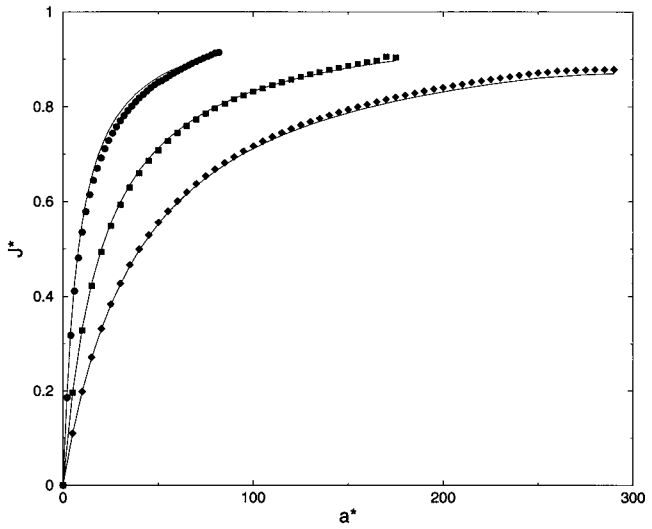

FIG. 1. Reduced current J^* as a function of the reduced applied field $a^*=E/E_T$. Circles, squares, and diamonds correspond to $\gamma^*=20$, 50, and 100, respectively. Solid lines are the theoretical predictions for the three values of γ^*. The grid size is $N=10\,000$.

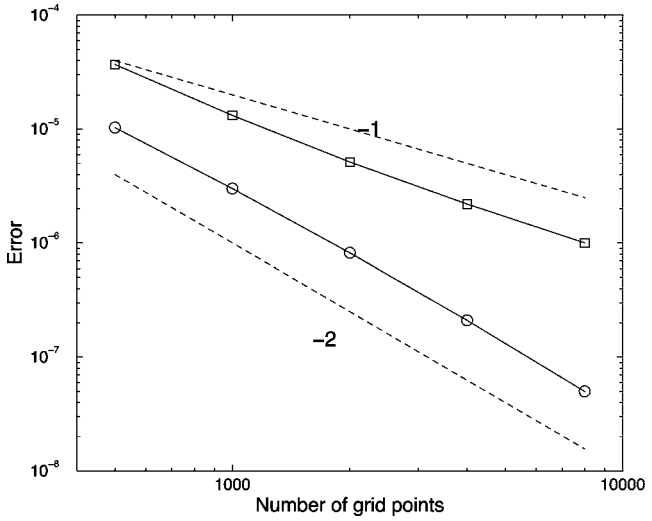

FIG. 2. The L_2 error of the numerical vs the analytical solution for the density and current, respectively, as a function of the number of grid points N at a given channel length L. The main parameters are $a^*=100$ and $\gamma^*=100$. The dashed lines correspond to N^{-1} and N^{-2} convergence.

figure, excellent agreement with the analytical solution (solid line) is appreciated not only in the linear Ohmic regime, but also in the strongly driven ($a^* \gg 1$) regime, where saturation effects dominate. We also note that the satisfactory agreement extends to the highly damped ($\gamma^* \gg 1$) regime relevant to nanofluidic applications. However, the full asymptotic limit, corresponding to an infinite drive, is never attained. In this regard, we observe that the maximum driving electric field is subject to a numerical stability constraint of the form $a\Delta t/\Delta x^2 \ll 1$, namely $a^* \ll 3N$, $N=L/\Delta x$ being the number of lattice sites in the simulation and $v_T^2=\frac{1}{3}$ in lattice units. By the same argument, the damping rate is subject to the stability constraint $\gamma \Delta t \ll 2$, namely $\gamma^* \ll 2N$. In view of these estimates, we observe that the present three-speed scheme still operates well below its linear stability limits. This is probably due to a combination of factors, that is, a limited number of discrete speeds, first-order time marching, as well as nonoptimized boundary conditions (see below).

Inspection of the (exponential) density profiles shows that the maximum error relative to the analytical solution is invariably associated with the density profile in the outlet layer, $L(1-1/a^*)<x<L$, where most of the spatial change takes place. This error is found to go from just a few percent for $a^* \sim O(10)$, up to 20% in the strongly driven regime, $a^* \sim O(100)$. This is probably caused by the representation of the reservoirs by a single lattice point. The consequences of a less abrupt treatment of the boundaries will be explored in the future. The global error, measured in L_2 norm, $E_2[\rho]=\sqrt{(1/N)\Sigma_{x=1}^{N}[\rho(x)-\rho_{exact}]^2}$ (and the same for the current J), shows a quadratic dependence for the density and intermediate linear-to-quadratic dependence for the current (see Fig. 2). Note that the absolute value of the errors remains acceptable.

In conclusion, the lattice FPE has been applied to the study of electrorheological transport of a one-dimensional charged fluid, and found to yield satisfactory agreement with a recent nontrivial analytical solution. In particular, the lattice FPE proves capable of predicting the saturation effect resulting from the nonlinear interaction between the electric field and the constant-flux boundary conditions imposed by the presence of equilibrium reservoirs at the channel boundaries. The present lattice FPE extends straightforwardly to higher dimensions and it might prove useful for the numerical investigation of more complex situations, such as heterogeneus channels with kinetic traps, and/or multicomponent fluids, for which analytical solutions are no longer available.

J.P.H. acknowledges the generous support of INFM while in Rome and the kind hospitality of G. Ciccotti and G. Parisi. S.M. and S.S. gratefully acknowledge kind hospitality and financial support by the Cambridge University. The authors are grateful to D. Moroni, B. Rotenberg, and A. Louis for useful comments and discussions.

APPENDIX A: DERIVATION OF THE LATTICE-FOKKER-PLANCK EQUATION

The lattice version of the kinetic equation (1) has been derived in a recent work [15], and therefore only the basic steps of the main procedure are reported here. The distribution function is expanded onto a Hermite basis

$$f(x,v;t)=\sum_{k=0}^{K} F_k(x;t)h_k(v)w(v), \tag{A1}$$

where $w(v)=(2\pi v_T^2)^{-1/2}e^{-v^2/2v_T^2}$ is the one-dimensional Hermite weight function, while $h_k(v)$ is the Hermite polynomial of order k. By substituting Eq. (A1) into the kinetic equation Eq. (1), and projecting upon the Hermite basis, one arrives at the moment equations

$$\partial_t F_k(x;t) + \partial_x G_k(x;t) = C_k(x;t), \tag{A2}$$

where

$$F_k(x;t) = \int_{-\infty}^{\infty} f(x,v;t)h_k(v)dv, \tag{A3}$$

$$G_k(x;t) = \int_{-\infty}^{\infty} vf(x,v;t)h_k(v)dv, \tag{A4}$$

$$C_k(x;t) = \int_{-\infty}^{\infty} C^{FP}[f(x,v;t)]h_k(v)dv, \tag{A5}$$

C^{FP} being the linear FP operator.

The next step is to evaluate the kinetic moments F_k, G_k, and C_k by the Gauss-Hermite quadrature. Noting that $f(x,v;t)/w(v)$ is a polynomial in v, the quadrature reads

$$F_k(x;t) = \sum_{i=0}^{G-1} \frac{f(x,v_i;t)}{w(v_i)} w_i h_k(v_i), \tag{A6}$$

where v_i and w_i are the nodes and weights of the quadrature. We observe that Eq. (A6) is exact for polynomials of degrees up to $(2G+1)$, so that, in principle, the lattice Fokker-Planck equation is equivalent to a system of $G+1$ moment equations.

Expressions similar to Eq. (A6) hold for G_k and C_k. Substituting these into Eq. (A2), and equating the coefficients of $h_k(v_i)$ on both sides of the resulting sum, one obtains the following set of equations

$$\partial_t f_i(x;t) + v_i \partial_x f_i(x;t) = c_i(x;t), \quad 0 \leqslant i \leqslant G-1. \tag{A7}$$

where the following identifications have been made

$$f_i(x;t) \equiv f(x,v_i;t)w_i/w(v_i), \tag{A8}$$

$$c_i(x;t) \equiv C^{FP}[f(x,v_i;t)]w_i/w(v_i). \tag{A9}$$

The discrete collision operator is entirely specified by the coefficients c_i defined by Eq. (A9). These can be computed from the spectral decomposition of the continuous operator $C^{FP}[f(x,v;t)]$ similar to Eq. (A1), i.e.,

$$C^{FP}(v_i) \equiv C^{FP}[f(x,v_i;t)] = \sum_{k=0}^{K} C_k(x;t)h_k(v_i)w(v_i). \tag{A10}$$

Knowledge of the spectral coefficients $C_k(x,t)$ allows the discrete coefficients $c_i(x;t)$ in Eq. (A9) to be calculated, thereby providing an operational definition of the discrete FP operator. To this purpose, we write

$$C_k(x,t) = \sum_l C_{kl} F_l(x,t), \tag{A11}$$

where the coefficients

$$C_{kl} = \int_{-\infty}^{\infty} dv h_k(v) C^{FP} w(v) h_l(v) \tag{A12}$$

provide the matrix representation of the collision operator C^{FP} in the Hermite basis set (not necessarily in diagonal form). By substituting (A11) and (A12) into (10), taking into account the relations (20)–(22), and writing $c_i = \Sigma_j c_{ij} f_j$, we finally obtain

$$c_{ij} = w_i \sum_{kl} A_{ki} C_{kl} A_{lj}, \tag{A13}$$

where $A_{ki} = h_k(v_i)/H_k$ are orthonormalized eigenvectors stemming from the Hermite polynomials $[H_k^2 = \Sigma_i w_i h_k(v_i) h_k(v_i)]$. Specific values of A_{ki} for practical implementations can be found in [17].

[1] R. Benzi, S. Succi, and M. Vergassola, Phys. Rep. **222**, 145 (1992).

[2] D. Wolf-Gladrow, *Lattice Gas Cellular Automata and Lattice Boltzmann Models* (Springer-Verlag, Berlin, 2000).

[3] S. Succi, *The Lattice Boltzmann Equation for Fluid Dynamics and Beyond* (Oxford University Press, Oxford, 2001).

[4] S. Chen and G. D. Doolen, Annu. Rev. Fluid Mech. **30**, 329 (1998).

[5] A. Ladd and R. Verberg, J. Stat. Phys. **104**, 1191 (2001).

[6] M. Cates *et al.*, J. Phys.: Condens. Matter **16**, S3903 (2004).

[7] N. van Kampen, *Stochastic Processes in Physics and Chemistry* (North-Holland, Amsterdam, 1981).

[8] H. Risken, *The Fokker-Planck Equation*, 2nd ed. (Springer-Verlag, Berlin, 1989).

[9] D. S. Zhang, G. W. Wei, D. J. Kouri, and D. K. Hoffman, Phys. Rev. E **56**, 1197 (1997).

[10] J. Fok, B. Guo, and T. Tang, Math. Comput. **71**, 1497 (2002).

[11] B. Hille, *Ionic Channels of Excitable Membranes*, 2nd ed. (Sinauer Associated, Sunderland, MD, 1992).

[12] J. Piasecki, R. J. Allen, and J.-P. Hansen, Phys. Rev. E **70**, 021105 (2004).

[13] D. Tieleman, P. Biggins, G. Smith, and M. Sansom, Q. Rev. Biol. **44**, 473 (2001).

[14] D. Chen and R. Eisenberg, Biophys. J. **64**, 1405 (1993).

[15] S. Succi, S. Melchionna, and J.-P. Hansen, Int. J. Mod. Phys. C (to be published).

[16] I. V. Karlin, A. Ferrante, and H. C. Öttinger, Europhys. Lett. **47**, 182 (1999).

[17] S. Ansumali, I. V. Karlin, and H. C. Öttinger, Europhys. Lett. **63**, 798 (2003).

[18] D. Moroni, B. Rotenberg, J.-P. Hansen, S. Succi, and S. Melchionna, e-print cond-mat/0512497.